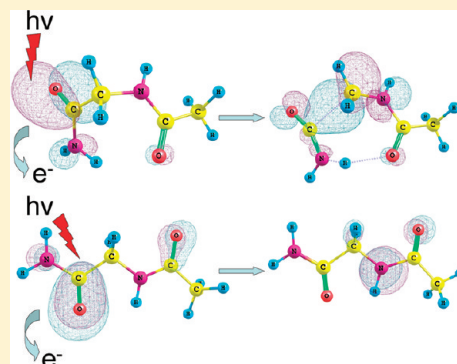


Influence of Turn (or Fold) and Local Charge in Fragmentation of the Peptide Analogue Molecule $\text{CH}_3\text{CO-Gly-NH}_2$ Following Single-Photon VUV (118.22 nm) Ionization

Atanu Bhattacharya[†] and Elliot R. Bernstein*

Department of Chemistry, Colorado State University, Fort Collins, Colorado 80523, United States

ABSTRACT: The radical cationic reactivity of the peptide analogue molecule $\text{CH}_3\text{CO-Gly-NH}_2$ is addressed both experimentally and theoretically. The radical cation intermediate of $\text{CH}_3\text{CO-Gly-NH}_2$ is created by single-photon ionization of this molecule at 118.22 nm (~ 10.5 eV). The two most stable conformers (C_7 and C_5) of this molecule exhibit different folds along the backbone: the C_7 conformer has a γ -turn structure, and the C_5 conformer has a β -strand structure. The experimental results show that the radical cation intermediate of $\text{CH}_3\text{CO-Gly-NH}_2$ dissociates and generates a fragment-ion signal at 73 amu that is observed through TOFMS. Theoretical results show how the fragment-ion signal at 73 amu is generated by only one conformer of $\text{CH}_3\text{CO-Gly-NH}_2$ (C_7) and how local charge and specific hydrogen bonding in the molecule influence fragmentation of the radical cation intermediate of $\text{CH}_3\text{CO-Gly-NH}_2$. The specific fold of the molecule controls fragmentation of this reactive radical cation intermediate. Whereas the radical cation of the C_7 conformer dissociates through a hydrogen-transfer mechanism followed by HNCO elimination, the radical cation of the C_5 conformer does not dissociate at all. CASSCF calculations show that positive charge in the radical cationic C_7 conformer is localized at the NH_2CO moiety of the molecular ion. This site-specific localization of the positive charge enhances the acidity of the terminal NH_2 group, facilitating hydrogen transfer from the NH_2 to the COCH_3 end of the molecular ion. Positive charge in the C_5 conformer of the $\text{CH}_3\text{CO-Gly-NH}_2$ radical cation is, however, localized at the COCH_3 end of the molecular ion, and this conformer does not have enough energy to surmount the energy barrier to dissociation on the ion potential energy surface. CASSCF results show that conformation-specific localization of charge in the $\text{CH}_3\text{CO-Gly-NH}_2$ molecular ion occurs as a result of the different hydrogen-bonding interactions involved in the different molecular conformers.



INTRODUCTION

Ionizing radiation and oxidative stress cause extensive damage to peptides through formation of their radical cation intermediates: these species are responsible for the development of a wide range of human physiological disorders.^{1,2} Therefore, understanding the reactivity of peptide radical cations is of considerable importance.^{3–11} Peptides are often found to fold into characteristic and functional three-dimensional structures,^{12–19} which are formed by hydrogen bonds bridging the hydrogen-bond acceptor CO and hydrogen-bond donor NH sites of different residues along the backbone in polypeptide chains. Several studies performed recently have revealed that these folds (or turns) in peptides play an important role in determining the reactivity of their radical cations.^{3–11}

Polypeptide chains can adopt different turns at different constituent amino acid residues. If an amino acid residue retains its identity in a peptide, then the local character of the amino acid residue governs the reactivity of the peptide. In this regard, therefore, understanding the reactivity of constituent amino acid residues involved in different turns in the peptide would be invaluable. Amino acid residues in a peptide can easily be modeled utilizing C- and N-terminus-protected amino acids, which contain peptide linkages ($-\text{CO}-\text{NH}-$) mimicking those

in the interior of a polypeptide chain. Therefore, a detailed characterization of the turn-specific reactivity of radical cation intermediates of C- and N-terminus-protected amino acids can easily untangle the local reactivity of peptide radical cations at a molecular level. Such studies, however, have not been systematically performed to date.

This article addresses the radical cation reactivity of the simplest peptide analogue molecule, $\text{CH}_3\text{CO-Gly-NH}_2$, whose structure is schematically illustrated in Figure 1. This molecule can form both a γ -turn and a β -strand through C_7 and C_5 hydrogen-bonding interactions, respectively (see Figure 1). Here, numbering of the atoms is done with respect to the hydrogen-bonded H atom in the hydrogen-bonding architecture. The conformer that forms a γ -turn through a C_7 hydrogen-bonding interaction is termed conformer C_7 , and the conformer that forms a β -strand through a C_5 hydrogen-bonding interaction is termed conformer C_5 . Herein, we address how these turns or hydrogen-bonding patterns influence the reactivity of the radical cation intermediate of $\text{CH}_3\text{CO-Gly-NH}_2$.

Received: April 27, 2011

Revised: August 23, 2011

Published: August 29, 2011

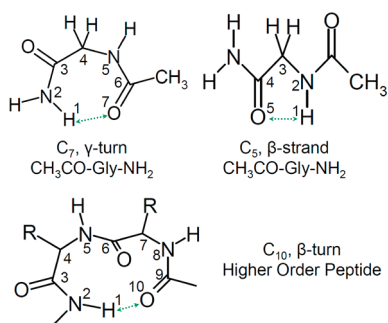


Figure 1. Schematics of different possible turns in the glycine-based peptide analogue molecule $\text{CH}_3\text{CO-Gly-NH}_2$. This molecule can have only a γ -turn and a β -strand, but cannot have a β -turn, which is possible only for higher-order peptides with more than one amino acid residue.

For unambiguous tracking of the turn-specific reactivity of the radical cationic intermediate of $\text{CH}_3\text{CO-Gly-NH}_2$, experimental trapping of conformers in their local minima is an essential prerequisite. Such an analysis can be implemented using a supersonic jet expansion following matrix-assisted laser desorption (MALD) to obtain an internal temperature low enough to suppress interconversion between different conformers of the neutral molecule. In this work, in situ generation of the radical cation intermediate of $\text{CH}_3\text{CO-Gly-NH}_2$ was performed through single-photon vacuum ultraviolet (VUV) ionization at 118.22 nm (~ 10.5 eV); fragmentation was monitored by linear time-of-flight mass spectrometry (TOFMS). The experimental studies were accompanied by highly correlated ab initio calculations at the MP2 and CASSCF levels of theory. This combined experimental and theoretical study is able to elucidate how the turn-specific hydrogen-bonding architecture and the specific localization of charge in the molecular ion control the radical cationic reactivity of $\text{CH}_3\text{CO-Gly-NH}_2$.

EXPERIMENTAL PROCEDURE

The experimental setup used to record time-of-flight mass spectrum was previously described in detail.²⁰ Briefly, the experimental setup consisted of a nanosecond laser system, a supersonic jet expansion nozzle with a laser desorption attachment, and a TOFMS chamber. The isolated gas-phase $\text{CH}_3\text{CO-Gly-NH}_2$ molecules were produced through a combination of MALD and supersonic jet expansion. The nozzle employed for the sample beam generation was constructed from a Jordan Co. pulsed valve and a laser desorption attachment.²¹ Sample drums for matrix desorption were prepared by wrapping a piece of porous filter paper around a clean aluminum drum. A solution of equimolar amounts of sample and matrix (R6G) in methanol was uniformly sprayed on the sample drum. An air atomizing spray nozzle (Spraying System Co.) with a siphon pressure of 10 psig was used to deposit $\text{CH}_3\text{CO-Gly-NH}_2$ and R6G on the drum surface. During the spraying, the drum was rotated and heated with a halogen lamp to ensure that the coating was homogeneous and dry. The dried sample drum was then placed in the laser ablation head/nozzle assembly and put into a vacuum chamber. To maintain fresh sample area for each laser ablation shot, a single motor was used to rotate and translate the sample drum simultaneously. $\text{CH}_3\text{CO-Gly-NH}_2$ molecules were desorbed from the drum by laser ablation at 532 nm, entrained in the flow of helium carrier gas through a 2 mm \times 60 mm channel in the ablation head, and expanded into the vacuum chamber.

In situ generation of the radical cation intermediate of $\text{CH}_3\text{CO-Gly-NH}_2$ was done using single-photon VUV ionization at 118.22 nm (~ 10.5 eV). The 118.22 nm radiation was the ninth harmonic of the fundamental output of a Nd:YAG laser at 1064 nm, and it was produced by focusing 354.67 nm radiation (third harmonic) from the Nd:YAG laser into a cell filled with Xe/Ar at a ratio of 1:10 at 200 Torr total pressure. A MgF_2 lens focused the 118.22 nm light into the ionization region of the TOFMS and dispersed the remaining 354.67 nm light. This dispersion of the 354.67 nm light ensured that molecular ionization in the ionization region of the TOFMS occurred entirely by 118.22 nm radiation.

The experiments were run at a repetition rate of 10 Hz. The timing sequence for the pulsed nozzle, ablation laser, and ionization laser was controlled by a time delay generator (SRS DG535). A background pressure of 1×10^{-5} Torr was maintained in the vacuum chamber during the experiment. Ion signals were detected by a microchannel plate detector (MCP). Each TOFMS spectrum was recorded by averaging the signal over 30 samples. Commercial $\text{CH}_3\text{CO-Gly-NH}_2$ (Aldrich) was used without any additional purification.

THEORETICAL METHODS

For rigorous descriptions of the potential energy surface (PES) of radical cation intermediates of biomolecules, highly correlated multiconfigurational methods are necessary.^{20(b)} Therefore, in the present work, exploration of cationic PESs was performed using the CASSCF level of theory. All geometry optimizations relevant to the ion-state decomposition of $\text{CH}_3\text{CO-Gly-NH}_2$ were carried out at the CASSCF(9,8)/6-31G(d) level of theory using the Gaussian 03²² programs. To explore the ion-state PESs, the active space comprised nine electrons distributed in eight orbitals, denoted as CASSCF(9,8). Only natural orbitals were considered. The orbitals used in this active space are illustrated in Figure 2. For conformer C_7 , the active orbitals included one O (COCH_3) nonbonding $2S_{\text{O}}$ orbital, two CO (COCH_3) σ -bonding and σ -antibonding orbitals (σ_{CO} , σ_{CO}^*), two CO (COCH_3) π -bonding and π -antibonding orbitals (π_{CO} , π_{CO}^*), two delocalized NCO (NH_2CO) π -bonding and π -antibonding orbitals (π_{NCO} , π_{NCO}^*), and one NCO (NH_2CO) π -nonbonding orbital $n\pi_{\text{NCO}}$. The active orbitals for conformer C_5 included one O (COCH_3) nonbonding $2S_{\text{O}}$ orbital, two CO (COCH_3) σ -bonding and σ -antibonding orbitals (σ_{CO} , σ_{CO}^*), two CO (NH_2CO) π -bonding and π -antibonding orbitals (π_{CO} , π_{CO}^*), two delocalized NCO (COCH_3) π -bonding and π -antibonding orbitals (π_{NCO} , π_{NCO}^*), and one NCO (COCH_3) π -nonbonding orbital $n\pi_{\text{NCO}}$.

All geometry optimizations were performed using a Berny optimization algorithm implemented in Gaussian 03 with default convergence criteria. The stability of the minimum-energy geometry was further confirmed by calculating analytical frequencies at the same level of theory. A true stable minimum should have no imaginary frequencies. Pathways in Figure 6 (below) were calculated using a relaxed scan optimization algorithm implemented in Gaussian 03. In this procedure, all geometrical parameters, except for the specified bond distance, were optimized, and electronic energy was monitored as the specified bond was elongated. Our previous work on amino acids including glycine revealed that, for the ion PES generated through valence ionization, a 6-31G(d) basis set is sufficient to describe the reaction pathways, if a proper active space for the CASSCF calculation is specified. If a larger basis set is used, computational cost increases

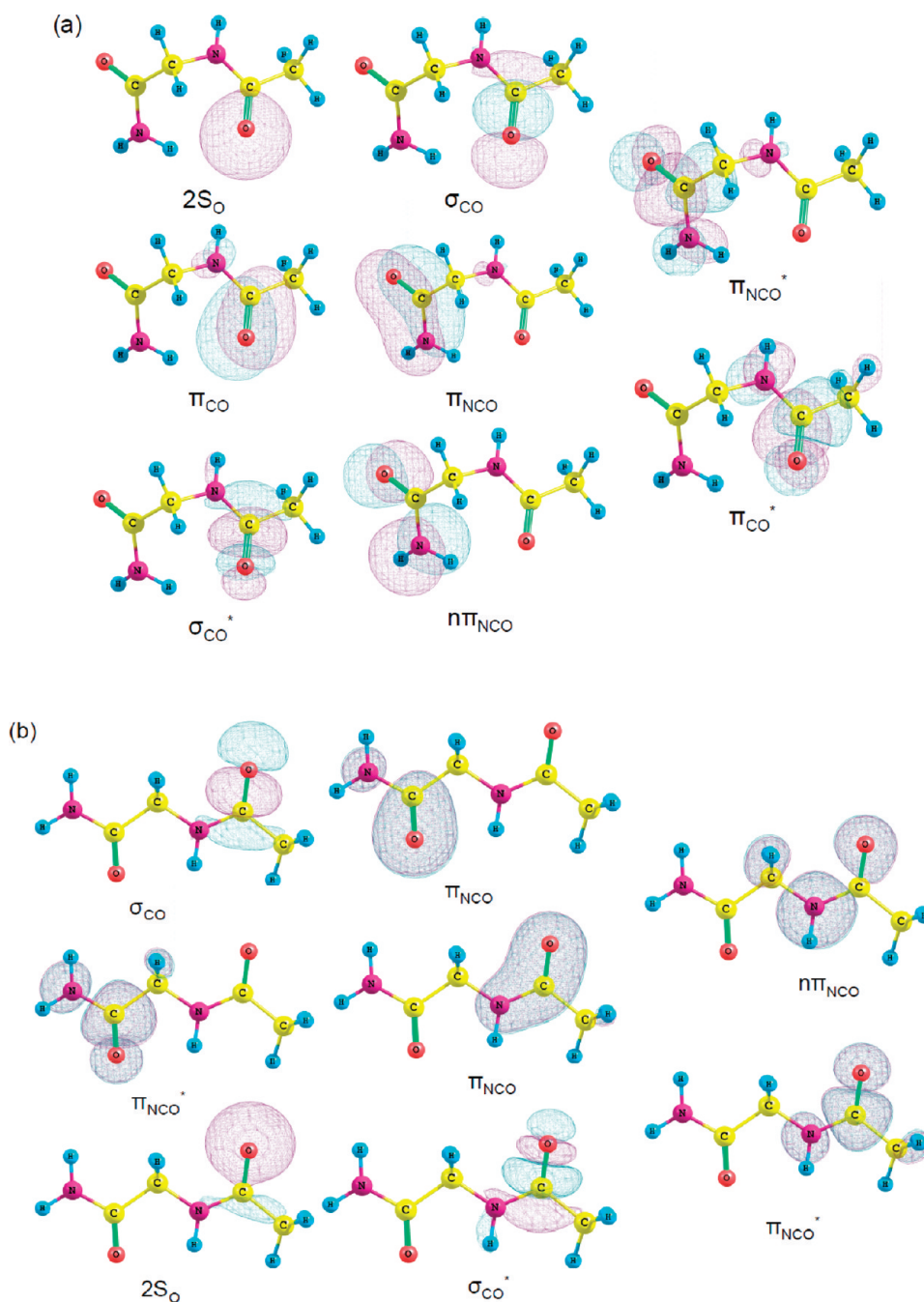


Figure 2. Active spaces used for (a) C_7 and (b) C_5 conformers of $\text{CH}_3\text{CO-Gly-NH}_2$ used in CASSCF calculations.

drastically; however, electronic energy does not change significantly. Therefore, a 6-31G(d) basis set was used for the present study. In fact, the MP2/aug-cc-pVDZ and CASSCF/6-31G(d) levels of theory predicted similar relative energies for C_7 and C_5 conformers in the same order. The present CASSCF computations were performed using 10 electrons distributed in 8 active orbitals for the neutral molecule and 9 electrons distributed in 8 active orbitals for the cation. This gives rise to 1176 configurations for the neutral and 2352 configurations for the cation. Selection of active orbitals was performed so that the same (or similar) orbitals were chosen for the two conformers.

We determined the lowest vertical ionization energy (VIE) by explicitly calculating the energy difference between neutral and

cation at the Franck–Condon geometry employing the MP2/aug-cc-pVDZ level of theory. Critical points (minima and transition states) are characterized by analytical frequency calculations. All calculations were executed at National Center for Supercomputing Application (NCSA). Optimized geometries and orbitals were visualized using Chemcraft software.

EXPERIMENTAL RESULTS

The two conformers C_7 and C_5 of neutral $\text{CH}_3\text{CO-Gly-NH}_2$ are schematically depicted in Figure 1. The conformers differ mainly by different types of intramolecular hydrogen-bonding linkages: $\text{N-H}\cdots\text{O}7=\text{C}$ (conformer C_7) and $\text{N-H}\cdots\text{O}5=\text{C}$

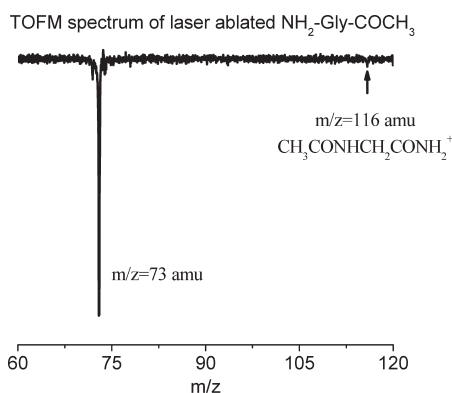


Figure 3. TOFMS spectrum of $\text{CH}_3\text{CO-Gly-NH}_2$ obtained through single-photon ionization at 118.22 nm (~ 10.5 eV).

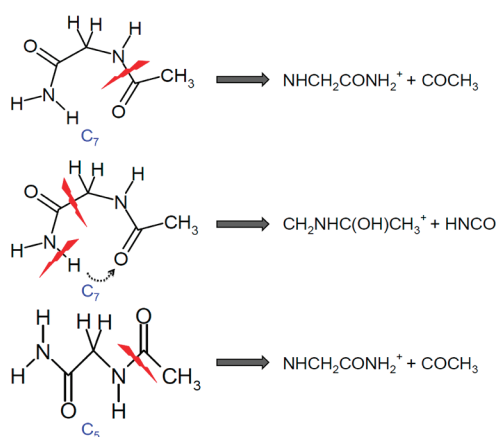


Figure 4. Possible decomposition schemes for two conformers of $\text{CH}_3\text{CO-Gly-NH}_2$ that can potentially generate fragment ions at $m/z = 73$ amu. They include COCH_3 elimination from either conformer C_7 or conformer C_5 (top and bottom) and hydrogen transfer from NH_2 to CO followed by HNCO elimination from conformer C_7 (middle).

(conformer C_5). Figure 3 shows the TOFMS spectrum of $\text{CH}_3\text{CO-Gly-NH}_2$ obtained through single-photon ionization at ~ 10.5 eV. The ion signal at $m/z = 116$ amu corresponds to the parent ion. The most intense ion signal at $m/z = 73$ amu is attributed to the fragment ion corresponding to either $\text{NHCH}_2\text{CONH}_2^+$ or $\text{CH}_2\text{NHC(OH)CH}_3^+$. This fragment ion can result from three possible decomposition pathways that are schematically shown in Figure 4. They include COCH_3 elimination from either conformer C_7 or C_5 , and hydrogen transfer from NH_2 to CO followed by HNCO elimination from conformer C_7 . The preferred fragmentation channel following ionization of $\text{CH}_3\text{CO-Gly-NH}_2$ was analyzed using theoretical calculations as discussed below.

In the present experiments, the isolated gas-phase $\text{CH}_3\text{CO-Gly-NH}_2$ molecules were produced through MALD. Although the MALD technique is a good method for placing easily fragmented, fragile molecules in the gas phase without fragmentation, great efforts are taken in the present work to ensure that $\text{CH}_3\text{CO-Gly-NH}_2$ was not fragmented during the ablation process.²¹ The arrival times for the fragment- and parent-ion signal intensities from laser ablation as a function of nozzle/pump laser timing were determined. Both fragment-ion and parent-ion signal intensities attenuated at the same nozzle timing; this suggests that the fragment ion was generated from the parent

molecule in the ionization region of the TOFMS instrument. If the fragmented species were generated by laser ablation at the ablation head attached to the pulsed nozzle, the parent-ion and fragment-ion signals would attenuate at different nozzle timings because of the difference in mass and size of the two species. This method demonstrates that fragment ion at 73 amu was generated in the ionization region of the TOFMS instrument, not in the laser desorption region of the nozzle. Moreover, many studies on aromatic substituted species (ionized at the local aromatic site) have been published for both peptides and amino acids, as well as sugars for which the same or similar MALD techniques have been employed and for which only the parent ion is observed.^{20h,23} Thus, MALD does not fragment biomolecules.

THEORETICAL RESULTS

The two lowest-energy conformers (C_7 and C_5) of neutral $\text{CH}_3\text{CO-Gly-NH}_2$ calculated at the CASSCF(10,8)/6-31G(d) level of theory are depicted in Figure 5a. Their zero-point-corrected relative electronic energy differences (in kcal/mol), calculated at both the CASSCF(10,8)/6-31G(d) and MP2/aug-cc-pVDZ levels of theory, are given in Table 1. The results presented in Table 1 show that conformer C_7 , which folds on its backbone through a γ -turn, represents the lowest-energy conformer of $\text{CH}_3\text{CO-Gly-NH}_2$. At the CASSCF(10,8)/6-31G(d) level of theory, the energy difference between the C_7 and C_5 conformers of $\text{CH}_3\text{CO-Gly-NH}_2$ was calculated to be 0.76 kcal/mol. The energy barrier for isomerization from C_7 to C_5 was calculated to be 4.1 kcal/mol at the MP2/aug-cc-pVDZ theory level. To surmount this rotational energy barrier, the temperature of the gas-phase molecules must be above ~ 50 K [considering $(3N - 6)RT$ cal/mol vibrational energy]. In the present experiments, the temperature of the molecular beam was estimated to be 5–10 K from the spectrum of NO .²¹ Therefore, the two conformers C_7 and C_5 are believed to be trapped in their local minima under the experimental conditions.

Although the energy difference between the C_7 and C_5 conformers was calculated to be only ~ 0.7 kcal/mol (which can be considered to be smaller than the best estimated value of numerical error), we believe that the two conformers of $\text{CH}_3\text{CO-Gly-NH}_2$ are not degenerate in energy: C_7 is more stable than C_5 for $\text{CH}_3\text{CO-Gly-NH}_2$, and they are separated by a 4.1 kcal/mol rotational energy barrier. Previously, Chin and co-workers²³ studied the structurally similar molecule $\text{CH}_3\text{CO-Phe-NH}_2$ experimentally using an IR–UV double-resonance approach. They found that conformer C_5 is most stable for $\text{CH}_3\text{CO-Phe-NH}_2$. The energy difference between these two conformers of $\text{CH}_3\text{CO-Phe-NH}_2$ was, however, calculated to be only 0.6 kcal/mol at the B3LYP/6-31G(d) theory level. Furthermore, the C_7 and C_5 conformers are the only two conformers that exhibit internal hydrogen bonding for the type of molecule discussed. Therefore, only these two conformers, C_5 and C_7 , are considered here. Furthermore, comparison of our work and Chin et al.'s²³ work suggests that the relative stability of the conformers of peptide analogue molecules depends entirely on the constituent amino acid residues and the inclusion of relatively bulky aromatic substituents.

Specific knowledge of the molecular-ion state produced upon sudden removal of an electron from a molecule is essential to determine the likely fragmentation mechanisms of the nascent radical cation. Gas-phase photoelectron spectroscopy can experimentally determine the vertical ionization energy (VIE) of a

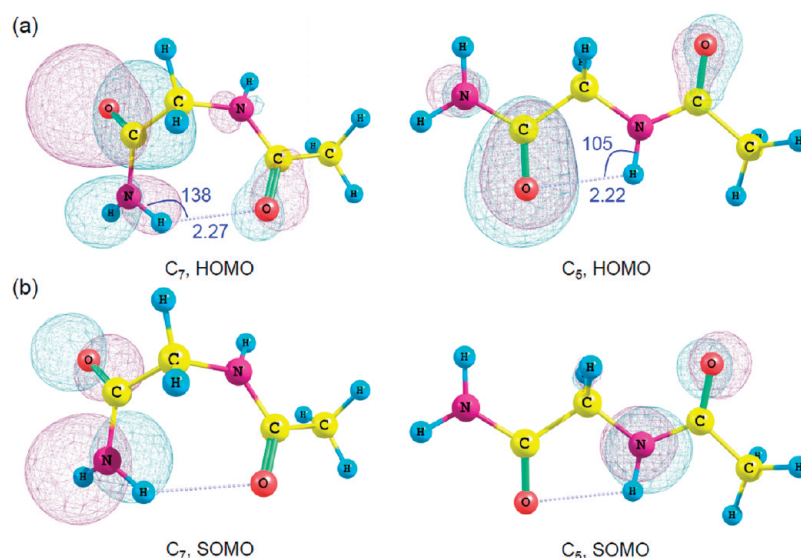


Figure 5. Two lowest-energy conformers (C_7 and C_5 involved in γ -turn and β -strand, respectively) of $\text{CH}_3\text{CO-Gly-NH}_2$ indicating their neutral S_0 stable structures calculated with CASSCF(10,8)/6-31G(d): (a) S_0 HOMO densities (CASSCF) for the two conformers and (b) D_0 SOMO densities. The HOMO and SOMO densities were calculated at the FC geometry. Important bond parameters are also included the figure.

Table 1. Relative Energies (kcal/mol) of the Two Lowest-Energy Conformers (C_7 and C_5) of Neutral $\text{CH}_3\text{CO-Gly-NH}_2$ Computed at the CASSCF(10,8)/6-31G(d) and MP2/aug-cc-pVDZ Levels of Theory

method	C_7	C_5
CASSCF(10,8)/6-31G(d)	0.00	0.76
MP2/aug-cc-pVDZ	0.00	0.60

molecule and the relevant ion state formed through photoionization. Gas-phase photoelectron spectroscopy of the $\text{CH}_3\text{CO-Gly-NH}_2$ molecule has not been recorded thus far, and therefore, we relied on theoretical calculations to determine the ionization energy of this molecule. Our previous work clearly demonstrated that MP2/aug-cc-pVDZ can successfully determine the first ionization energy for glycine.^{20b} As $\text{CH}_3\text{CO-Gly-NH}_2$ is a peptide analogue molecule of glycine, the MP2/aug-cc-pVDZ methodology should also be able to determine the ionization energy of $\text{CH}_3\text{CO-Gly-NH}_2$ with adequate accuracy.

The first VIEs for conformers C_7 and C_5 of $\text{CH}_3\text{CO-Gly-NH}_2$ were calculated to be 9.5 and 9.7 eV, respectively, at the MP2/aug-cc-pVDZ level of theory. The VIEs of the respective conformers were calculated by subtracting electronic energies of the ground S_0 and D_0 states at their Franck–Condon (FC) geometries, optimized at the same level of theory. Therefore, the above calculations suggest that single-photon ionization of $\text{CH}_3\text{CO-Gly-NH}_2$ at ~ 10.5 eV (118.22 nm) used in the experiment promotes the molecule to the D_0 ground ion state. Furthermore, almost 1 eV of excess energy is removed by the escaping photoelectron as kinetic energy when the molecular ion is formed at the FC region of the D_0 ground-state ion PES.

Following sudden removal of an electron from a neutral molecule, the nascent radical cation is typically not formed in its equilibrium geometry. On the several-hundred-femtosecond time scale, the molecular ion (called vertical ion or VI) generated at the FC region will evolve to the adiabatic ion (AI) while lowering its electronic potential energy through structural rearrangement/hydrogen transfer. Excess energy ($E_{\text{VI}} - E_{\text{AI}}$)

due to vertical-to-adiabatic evolution is stored in the vibrations of the bonds of the molecular ion under isolated conditions; this excess vibrational energy can cause the dissociation of the radical cation. The dissociation reaction for the D_0 ion is likely to occur through the lowest activation barrier. As a result, the energy barrier to the transition state to form a particular product becomes an important consideration for understanding the reactivity of the molecular ion.

The most intense fragment-ion signal at 73 amu observed experimentally corresponds to either $\text{NHCH}_2\text{CONH}_2^+$ or $\text{CH}_2\text{NHC(OH)CH}_3^+$, which can potentially be generated through three possible decomposition mechanisms as discussed previously and depicted in Figure 4. Therefore, we first considered the theoretical exploration of all three channels of decomposition at the CASSCF(9,8)/6-31G(d) level of theory to judge which of them is energetically more favorable. Although the MP2/aug-cc-pVDZ level of theory was employed to determine the ionization energy of $\text{CH}_3\text{CO-Gly-NH}_2$, for exploration of the D_0 PES of the radical cation $\text{CH}_3\text{CO-Gly-NH}_2$, the CASSCF methodology was employed. A number of electronic configurations usually contribute to a particular radical cationic state, and “near-degeneracy effects”, caused by the presence of conical intersections between the many low-lying valence cationic states, become particularly important. Monoconfigurational methods, such as MP2, often over- or underestimate the energy barrier to a transition state on the ground PES of a radical cation. Illustrations of such considerations were found recently for many organic compounds²⁴ and in our previous work.^{20b} Therefore, exploration of radical cationic PESs of C_7 and C_5 conformers of $\text{CH}_3\text{CO-Gly-NH}_2$ was performed using the CASSCF level of theory, which can take account of both near-degeneracy effects and multiple electronic configurations.

The potential energy diagrams associated with simple C–N bond dissociation (or, equivalently, COCH_3 elimination) for the C_7 and C_5 conformers of radical cationic $\text{CH}_3\text{CO-Gly-NH}_2$ on the D_0 surface, obtained at the CASSCF(9,8)/6-31G(d) level of theory, are shown in Figure 6. The MP2 energy profile is also included in the figure for comparison. This figure illustrates that

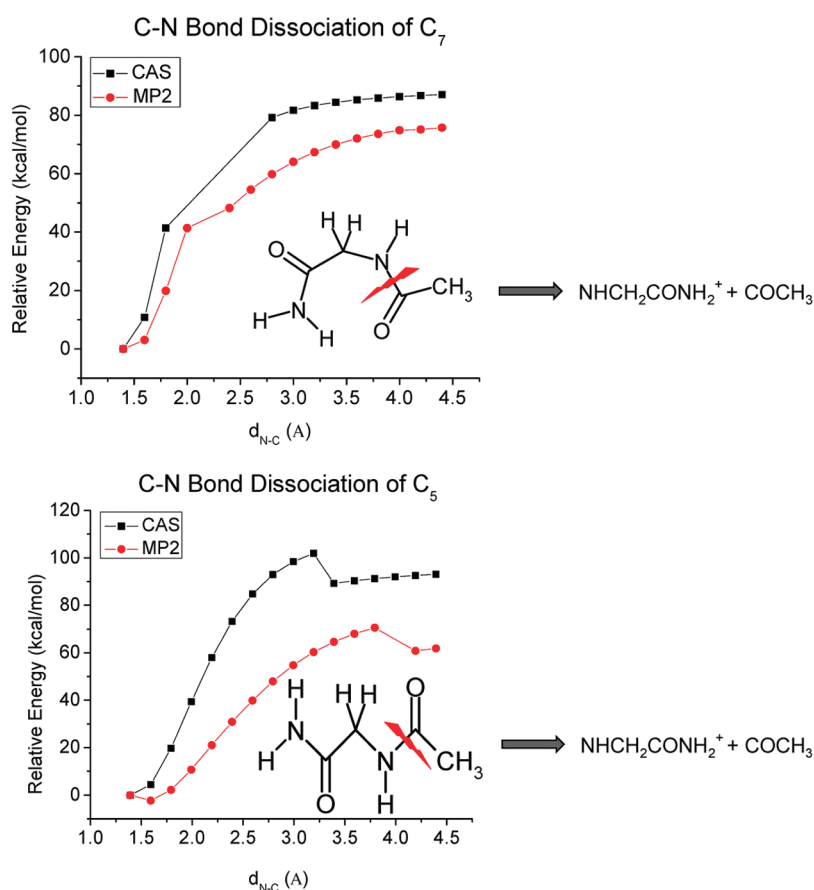


Figure 6. D_0 PES scans associated with the COCH_3 elimination pathway for C_7 (top) and C_5 (bottom) conformers of $\text{CH}_3\text{CO-Gly-NH}_2$, computed at the CASSCF/6-31G(d) level of theory. Note that this COCH_3 elimination pathway can potentially generate fragment-ion signal at $m/z = 73$ amu corresponding to $\text{NHCH}_2\text{CONH}_2^+$. The units for the X axis are angstroms. The sudden drop in energy for the C–N bond dissociation arises because of the step size used for the PES scan. If a smaller step size were used, a smoother change in energy could be rendered.

the simple COCH_3 elimination reaction on the D_0 surface is associated with activation barriers of ~ 80 and ~ 100 kcal/mol for the C_7 and C_5 conformers, respectively, with respect to their D_0 FC points. Therefore, the simple COCH_3 elimination channel is not accessible for both the C_7 and C_5 conformers following single-photon ionization of $\text{CH}_3\text{CO-Gly-NH}_2$ at ~ 10.5 eV. This photoionization procedure promotes the molecule to the FC point of the D_0 ground-state ion PES with no excess energy for surmounting a barrier of 80–100 kcal/mol.

Figure 7a shows the PE diagram associated with hydrogen transfer from the NH_2 to COCH_3 group, followed by HNCO elimination for conformer C_7 , predicted at the CAS(9,8)/6-31G(d) level of theory. Figure 7b depicts the unstable normal mode of vibration associated with the HNCO elimination transition state. The hydrogen-transfer process stores an energy of 14.86 kcal/mol in molecular vibrations, whereas subsequent HNCO elimination requires an energy of 12.56 kcal/mol. Thus, hydrogen transfer followed by HNCO elimination is an energetically allowed process from the FC point on the C_7 D_0 PES. Clearly, the present theoretical results lead to the conclusion that the C_7 conformer of $\text{CH}_3\text{CO-Gly-NH}_2$ at the FC point on the D_0 PES will dissociate by the pathway involving hydrogen transfer followed by HNCO elimination. The other pathway, the COCH_3 elimination channel, as mentioned above, is inaccessible for both C_7 and C_5 conformers. Thus, the fragment-ion signal at $m/z = 73$ amu arises from $\text{CH}_2\text{NHC(OH)CH}_3^+$, rather than $\text{NHCH}_2\text{CONH}_2^+$.

Figure 8 shows the PE diagram associated with VI-to-AI relaxation and subsequent hydrogen transfer for conformer C_5 on its D_0 ion PES calculated at the CASSCF(9,8)/6-31G(d) level of theory. This figure shows that molecular ion C_5 undergoes a slight geometrical change while evolving from VI to AI1. This VI-to-AI evolution stores energy of 8 kcal/mol in molecular vibration; however, the subsequent hydrogen-transfer pathway needs to surmount an activation barrier of 13.45 kcal/mol. Therefore, the C_5 molecular ion is expected to be trapped on its cationic PES: conformer C_5 is thus stable on its D_0 ion surface and not prone to molecular fragmentation, in contrast to conformer C_7 .

When a molecule is ionized, a hole (electron deficiency) is created in the molecule electron density, rendering a radical cation. The reactivity of the radical cation intermediate of biomolecules such as amino acids, lactic acid, and pyruvic acid was previously found to be determined by the specific localization of the electron density hole in the molecular ion.^{20b} A similar situation arises for the present case of the model peptide radical cation $\text{CH}_3\text{CO-Gly-NH}_2^+$: Following single-photon ionization at ~ 10.5 eV, a strong correlation is found between reactivity and specific localization of a hole density or positive charge in the radical cation.

In the simplest view of electronic structure theory, ionization is removal of an electron from an orbital that was occupied in the neutral parent molecule. Therefore, under a restricted scheme in which each molecular orbital of a neutral species is considered to contain two electrons, according to Koopmans' theorem,²⁵ the

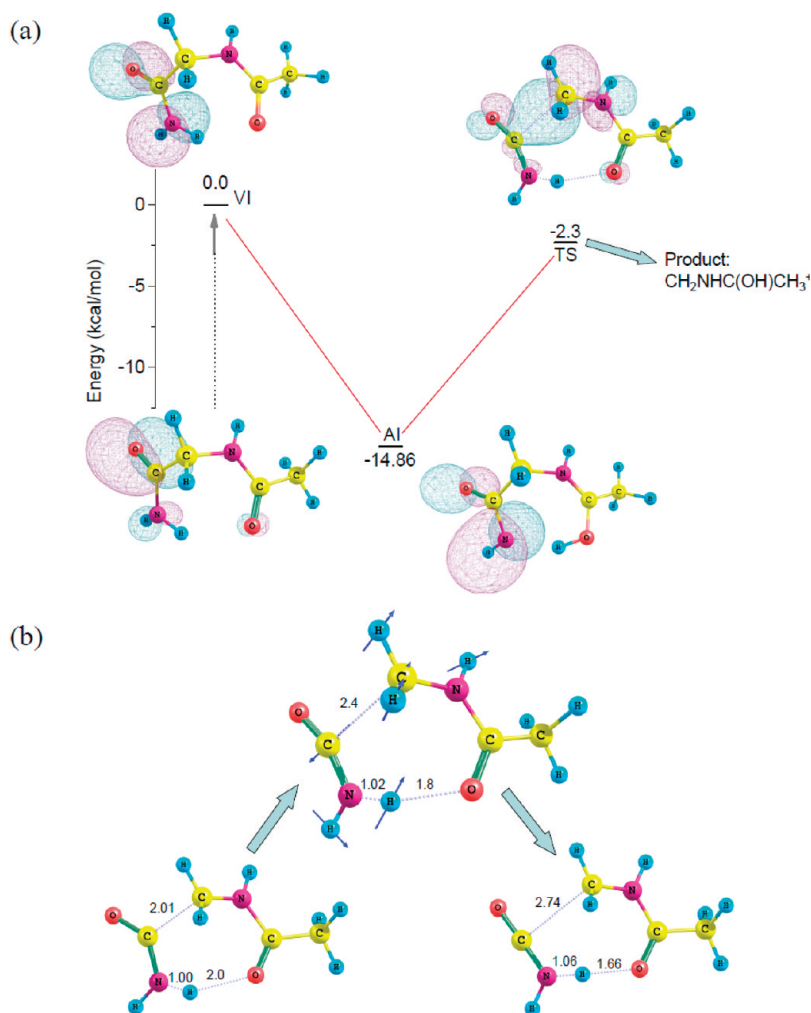


Figure 7. (a) PE diagram associated with elimination of HNC(O) to generate $\text{H}_3\text{C}(\text{OH})\text{NHCH}_2^+$ (73 amu) for conformer C_7 , computed at the CASSCF(9,8)/6-31G(d) level of theory. (b) Unstable normal mode of vibration associated with TS in the figure along with relevant geometrical changes associated with the vibration to ensure that the TS is connected with the HNC(O) elimination pathway.

first ionization energy corresponds to the energy required to remove an electron from the highest occupied molecular orbital (HOMO) of a neutral molecule. This ionization creates a hole in the molecular electronic distribution that resides in the singly occupied molecular orbital (SOMO) of the nascent radical cation. The SOMO under this restricted scheme, represents the single-electron density distribution or hole density distribution in the nascent molecular cation. Knowledge of the hole density distribution for different conformers of radical cationic $\text{CH}_3\text{CO-Gly-NH}_2$ is important to understand its reactivity at a molecular level.

Electron density distributions associated with each orbital can be generated easily by depicting the spatial function of a paired spin-orbital. Toward this end, a spatial function using CASSCF theory was created, incorporating natural orbitals as an initial guess obtained from the optimized geometry on the ion-state surface for each conformer of $\text{CH}_3\text{CO-Gly-NH}_2$. The electron density distribution for the HOMO and hole density distribution for the SOMO of conformer C_7 of $\text{CH}_3\text{CO-Gly-NH}_2$ at the FC point [CASSCF(10,8)/6-31G(d)-optimized geometry] are shown in Figure 5a,b. The two colors indicate the plus and minus phases of the wave functions. For conformers C_7 and C_5 of

neutral S_0 $\text{CH}_3\text{CO-Gly-NH}_2$, the HOMO is localized on the NH_2CO end of the molecule, notably in a π_{CO} bonding orbital. The SOMO for conformer C_7 is also localized on the NH_2CO end of the molecular ion; however, it is mostly in an $n\pi_{\text{NCO}}$ non-bonding orbital. Therefore, CASSCF calculations predict that, if an electron is removed from the HOMO of the C_7 conformer, a hole is initially localized at the NH_2CO end of the molecule. Immediately (physically, at zero time delay) after ionization, the hole still resides in the neutral HOMO; however, because of the reduced number of electrons in the molecular ion following ionization, the mean field of the electrons is changed: thereby, the electronic distribution of the molecular ion is reorganized (within the attosecond time scale). The nuclei do not move on this time scale, and the FC geometry of the molecule is still unaltered on the ion surface. Once the final electronic distribution is established at the FC geometry on the molecular ion PES, the SOMO represents the current hole density distribution for the molecular ion. CASSCF calculations predict that the C_7 conformer SOMO is localized at the same NH_2CO end of the molecule, but a change in spatial distribution of the hole density occurs because of electron–electron correlation on ion-state surface.

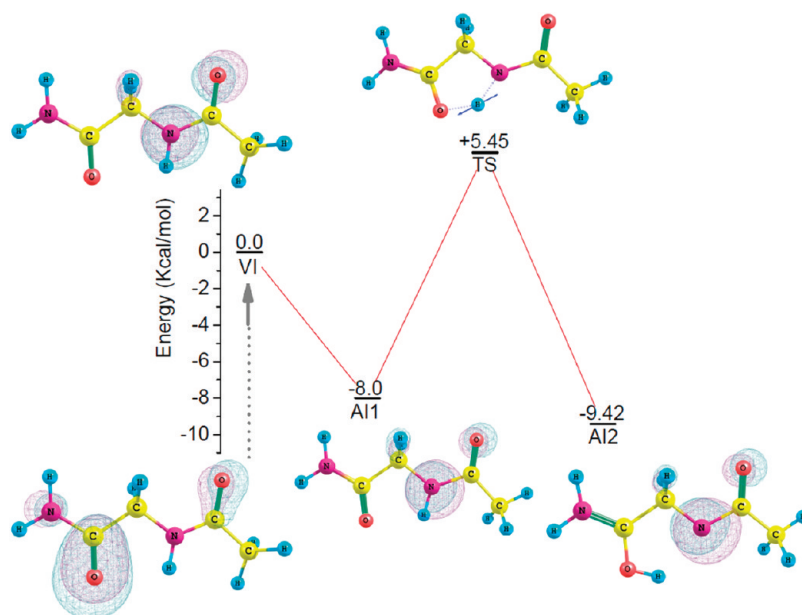


Figure 8. PE diagram associated with vertical to adiabatic evolution and hydrogen-transfer pathway for the C_5 conformer on the D_0 ion-state surface, computed at the CASSCF(9,8)/6-31G(d) level of theory.

In contrast, Figure 5 shows that the electron density distribution for the HOMO and hole density distribution for the SOMO of the C_5 conformer at the FC point for the respective surfaces (calculated at the CASSCF level of theory) are localized at the two different ends of the molecule: the SOMO is localized on the COCH_3 end of the molecule, and the HOMO is localized on the NH_2CO end of the molecule. The HOMO represents a π_{CO} bonding orbital, and the SOMO represents an $n\pi_{\text{NCO}}$ nonbonding orbital. Thus, the CASSCF methodology indicates that, upon photoionization of conformer C_5 at ~ 10.5 eV, a hole is created at the NH_2CO end of the molecule, which eventually undergoes ultrafast (attosecond) charge migration to the other COCH_3 end of the molecule. On the other hand, the hole resides at the same end of the molecular ion for conformer C_7 .

Similar hole migration, as addressed above, from one end to the other end of polypeptides in the C_5 conformation was previously computationally predicted by Levine and co-workers.²⁶ Our present work shows that, if a peptide chain is folded, such an ultrafast charge migration can be hindered. In particular, the C_5 conformer of $\text{CH}_3\text{CO-Gly-NH}_2$ facilitates charge migration from the NH_2CO end to the COCH_3 end of the molecule, but conformer C_7 , which has a γ -folded geometry, hinders charge migration and is prone to fragmentation. The γ -turn of the C_7 conformer then leaves the $\text{CH}_3\text{CO-Gly-NH}_2$ model peptide prone to fragmentation, whereas the β -strand geometry of the C_5 conformer suppresses fragmentation.

Usually, following generation of a radical cation, the bond that breaks is the one at which the hole in the electron density (reduced electron density) is ultimately localized in the molecular ion. For conformer C_7 , the SOMO is entirely localized at the NH_2CO end, and for conformer C_5 , the SOMO is localized at the COCH_3 end of the molecular ion. The hole in the NH_2CO group electron density is thereby predicted to facilitate hydrogen transfer from the NH_2 group to the COCH_3 group. Following hydrogen transfer, the SOMO hole density distribution at the transition-state geometry of the C_7 conformer associated with HNCO elimination (see Figure 7) becomes localized in the

C-N bond of the molecule. As a result, this facilitates the HNCO elimination channel, as the C-C bond weakens. Thus, in this case, the reactivity of radical cationic $\text{CH}_3\text{CO-Gly-NH}_2$ is correlated with the hole density distributions. We propose that the chemistry of such a reactive intermediate of the peptide analogue molecule $\text{CH}_3\text{CO-Gly-NH}_2$ is determined by its conformations (or folds) and specific localization of charge in the molecule. This can be generalized for longer polypeptide systems.

DISCUSSION

A number of observations are crucial for understanding the reactivity of the radical cation intermediate of $\text{CH}_3\text{CO-Gly-NH}_2$ generated following photoionization of the molecule at ~ 10.5 eV. Undoubtedly, if the excess energy, obtained through the vertical-to-adiabatic evolution of the molecular ion on its D_0 cationic PES, is sufficient to surmount the activation energy needed to initiate a decomposition reaction, fragmentation of this radical cation intermediate takes place. Theoretical computations at the MP2 level of theory predict that single-photon VUV ionization of $\text{CH}_3\text{CO-Gly-NH}_2$ at ~ 10.5 eV excites the molecules to the FC region of the D_0 ground-state ion. CASSCF results show that the excess energy stored in the C_7 conformer molecular ion due to vertical-to-adiabatic evolution is around 14.86 kcal/mol. With this excess energy, this most stable conformer C_7 can dissociate through the HNCO elimination channel because this elimination channel requires only 12.56 kcal/mol to surmount the appropriate energy barrier (see Figure 7a). This pathway generates the fragment-ion signal at 73 amu in TOFMS measurements, which corresponds to the $\text{CH}_2\text{NHC(OH)CH}_3^+$ fragment ion. Other relevant decomposition channels, such as COCH_3 elimination, which can also potentially generate the same fragment from both the C_7 and C_5 conformers, are associated with high activation barriers (≥ 14.56 kcal/mol; see Figure 6) and, therefore, are not accessible from the FC point of the ion D_0 PES. Decomposition of the peptide analogue molecule $\text{CH}_3\text{CO-Gly-NH}_2$ studied here is controlled by its specific

conformation. Only conformer C_7 dissociates; conformer C_5 does not dissociate at the ionization energy (~ 10.5 eV corresponding to 118.22 nm) used in the present study.

Theoretical results also demonstrate that, for conformer C_7 , both the HOMO and SOMO are localized at the NH_2CO end of the molecular ion. The HOMO and SOMO for this conformer at its FC geometry are essentially π_{CO} and $n\pi_{\text{NCO}}$ orbitals, respectively. This localization of electron hole density at the CONH_2 group facilitates hydrogen transfer followed by NHCO elimination for conformer C_7 . The HOMO and SOMO of conformer C_5 , on the other hand, are localized at different ends of the molecular ion at its FC geometry. The HOMO of conformer C_5 represents a π_{CO} orbital at the NH_2CO end of the molecule, whereas the SOMO represents an $n\pi_{\text{NCO}}$ orbital at the COCH_3 end of the molecule. This suggests that an ultrafast (attosecond) charge migration occurs in conformer C_5 immediately following its photoionization at ~ 10.5 eV. Therefore, the localization site for the hole of conformer C_7 and C_5 of $\text{CH}_3\text{CO-Gly-NH}_2$ on the D_0 ion PES is clearly conformation-specific. Furthermore, the hydrogen bond involved in the γ -turn for conformer C_7 enhances the reactivity of its radical cation intermediate, providing a direct pathway for hydrogen transfer and subsequent NHCO elimination. Conformer C_5 does not dissociate, which, in turn, renders its molecular ion stable. Thus, the reactivity of the radical cation intermediate of $\text{CH}_3\text{CO-Gly-NH}_2$ is directed by two specific properties of the molecular ion: (1) specific localization of charge and (2) initial intramolecular hydrogen bond involved in different turns or folds.

The ionization cross sections for the C_7 and C_5 parent conformers are not known and could be quite different. The relative population distributions of these two conformers in molecular beams could also be quite different from Boltzmann population distributions because, during fast adiabatic cooling, the conformers are trapped in their local minima that are separated by a large energy barrier. Therefore, although a mixture of the two conformers is present in the molecular beam and only the C_7 conformer dissociates to generate fragment-ion signal at 73 amu, only a small amount of the parent ion that is generated because of the presence of conformer C_5 is left. To determine the relative abundances of the two conformers from the mass spectrum given in this article, one must consider the relative populations, as well as ionization cross sections for both C_5 and C_7 conformers.

CONCLUSIONS

This article addresses a study of the radical cation intermediate chemistry of the simplest peptide analogue molecule, $\text{CH}_3\text{CO-Gly-NH}_2$. This molecule can exist in different structural forms: γ -folded with a C_7 hydrogen-bonding interaction and unfolded (β -strand) with a C_5 intramolecular hydrogen-bonding interaction. Only the γ -folded form dissociates through hydrogen transfer from the NH_2 to COCH_3 group followed by HNCO elimination subsequent to single-photon ionization at ~ 10.5 eV. This pathway results in the fragment-ion signal at 73 amu, which corresponds to $\text{CH}_2\text{NHC(OH)CH}_3^+$. The reason for this turn-specific fragmentation behavior is localization of positive charge at the NH_2CO moiety of conformer C_7 . This electron density hole localization enhances the acidity of the NH_2 group. The radical cation of conformer C_5 is computationally predicted to be stable under these conditions: it does not dissociate at all with the excess energy obtained through single-photon ionization at ~ 10.5 eV. Thus, molecular folding of the model peptide

$\text{CH}_3\text{CO-Gly-NH}_2$ plays an important role in determining the reactivity of its radical cation.

In this study, the MALD technique was successfully employed to explore the photoionization behavior of the simplest peptide analogue molecule $\text{CH}_3\text{CO-Gly-NH}_2$. The same technique can be employed to study dipeptides, tripeptides, and so on. To study the role of folding for the reactivity of isolated peptides, IR–VUV photoionization spectroscopy would be extremely advantageous, as this spectroscopic approach can directly demonstrate how different fragments are connected to different turn-specific conformers. Selective deuteration of the CH_3 end, as well as the NH_2 end of the molecule, and substitution of $\text{N}(\text{CH}_3)_2$ instead of NH_2 would be helpful in further exploring the radical cationic intermediate chemistry of peptide analogue molecules. In a broader sense, the present study predicts that, following formation of radical cation intermediates of proteins, because of the effect of ionizing radiation and/or oxidative stress, some folds of a protein might be reactive and others might not. Therefore, by changing the folding of a protein, one can, in principle, control the reactivity of its radical cation intermediate.

AUTHOR INFORMATION

Corresponding Author

*E-mail: erb@lamar.colostate.edu.

Present Addresses

[†]Chemistry Department, Brookhaven National Laboratory, Upton, NY 11973.

ACKNOWLEDGMENT

We thank the NCSA TERAGRID and the U.S. Army Research Office (ARO) for support of this research.

REFERENCES

- (1) Kantorow, M.; Hawse, J. R.; Cowell, T. L.; Benhamed, S.; Pizarro, G. O.; Reddy, V. N.; Heijtmancik, J. F. *Proc. Natl. Acad. Sci. U.S.A.* **2004**, *101*, 9654–9659.
- (2) (a) Varadarajan, S.; Yatin, S.; Kansj, J.; Jahanshahi, F. *Brain Res. Bull.* **1999**, *50*, 133–141. (b) Schoneich, C.; Pogocki, D.; Hug, G. L.; Bobrowski, K. *J. Am. Chem. Soc.* **2003**, *125*, 13700–13713. (c) Yashiro, H.; White, R. C.; Yurkovskaya, A. V.; Forbes, M. D. E. *J. Phys. Chem. A* **2005**, *109*, 5855–5864.
- (3) Chu, I. K.; Zhao, J.; Xu, M.; Siu, S. O.; Hopkinson, A. C.; Siu, K. W. M. *J. Am. Chem. Soc.* **2008**, *130*, 7862.
- (4) Chu, I. K.; Rodriguez, C. F.; Lau, T.; Hopkinson, A. C.; Siu, K. W. M. *J. Phys. Chem. B* **2000**, *104*, 3393.
- (5) Bagheri-Majidi, E.; Ke, Y.; Orlova, G.; Chu, I. K.; Hopkinson, A. C.; Siu, K. W. M. *J. Phys. Chem. B* **2004**, *108*, 11170.
- (6) Barlow, C. K.; Wee, S.; McFadyen, W. D.; O'Hair, R. A. J. *Dalton Trans* **2004**, *20*, 3199.
- (7) Chu, I. K.; Rodriguez, C. F.; Hopkinson, A. C.; Siu, K. W. M.; Lau, T.-C. *J. Am. Soc. Mass Spectrom.* **2001**, *12*, 1114.
- (8) O'Hair, R. A. J.; Blanksby, S.; Styles, M.; Bowie, J. H. *Int. J. Mass Spectrom.* **1999**, *182*, 203.
- (9) Turecek, F.; Carpenter, F. H.; Polce, M. J.; Wesdemiotis, C. *J. Am. Chem. Soc.* **1999**, *121*, 7955.
- (10) Polce, M. J.; Wesdemiotis, C. *J. Am. Soc. Mass Spectrom.* **1999**, *10*, 1241.
- (11) (a) Stubbe, J.; van der Donk, W. A. *Chem. Rev.* **1998**, *98*, 705. (b) Berlett, B. S.; Stadtman, E. R. *J. Biol. Chem.* **1997**, *272*, 20313. (c) Stadtman, E. R. *Annu. Rev. Biochem.* **1993**, *62*, 797.
- (12) Branden, C.; Tooze, J. *Introduction to Protein Structure*; Garland Publishing: New York, 1999.

- (13) Toniolo, C. *CRC Crit. Rev. Biochem.* **1980**, *9*, 1.
- (14) Smith, J. A.; Pease, L. G. *CRC Crit. Rev. Biochem.* **1980**, *8*, 314.
- (15) Milner-White, E. J. *J. Mol. Biol.* **1990**, *216*, 385.
- (16) Hutchinson, E. G.; Thornton, J. M. *Protein Sci.* **1994**, *3*, 2209.
- (17) Chou, K. *Anal. Biochem.* **2000**, *286*, 1.
- (18) Guruprasad, K.; Rajkumar, S. *J. Biosci.* **2000**, *25*, 143.
- (19) Guruprasad, K.; Prasad, M. S.; Kumar, G. R. *J. Pept. Res.* **2001**, *57*, 292.
- (20) (a) Hu, Y. J.; Bernstein, E. R. *J. Chem. Phys.* **2008**, *128*, 164311. (b) Bhattacharya, A.; Shin, J.-W.; Clawson, K. J.; Bernstein, E. R. *Phys. Chem. Chem. Phys.* **2010**, *12*, 9700. (c) Hu, Y. J.; Fu, H. B.; Bernstein, E. R. *J. Chem. Phys.* **2006**, *125*, 184308. (d) Hu, Y. J.; Fu, H. B.; Bernstein, E. R. *J. Chem. Phys.* **2006**, *125*, 184308. (e) Hu, Y. J.; Fu, H. B.; Bernstein, E. R. *J. Chem. Phys.* **2006**, *125*, 154306. (f) Hu, Y. J.; Fu, H. B.; Bernstein, E. R. *J. Chem. Phys.* **2006**, *124*, 024302. (g) Hu, Y. J.; Fu, H. B.; Bernstein, E. R. *J. Chem. Phys.* **2006**, *125*, 154305. (h) Shin, J.-W.; Bernstein, E. R. *J. Chem. Phys.* **2009**, *130*, 214306. (i) Shin, J.-W.; Dong, F.; Grisham, M. E.; Rocca, J. J.; Bernstein, E. R. *Chem. Phys. Lett.* **2011**, *506*, 161.
- (21) Im, H.-S.; Bernstein, E. R. *J. Chem. Phys.* **2000**, *113*, 7911.
- (22) Frisch, M. J.; Trucks, G. W.; Schlegel, H. B.; Scuseria, G. E.; Robb, M. A.; Cheeseman, J. R.; Montgomery, J. A., Jr.; Vreven, T.; Kudin, K. N.; Burant, J. C.; Millam, J. M.; Iyengar, S. S.; Tomasi, J.; Barone, V.; Mennucci, B.; Cossi, M.; Scalmani, G.; Rega, N.; Petersson, G. A.; Nakatsuji, H.; Hada, M.; Ehara, M.; Toyota, K.; Fukuda, R.; Hasegawa, J.; Ishida, M.; Nakajima, T.; Honda, Y.; Kitao, O.; Nakai, H.; Klene, M.; Li, X.; Knox, J. E.; Hratchian, H. P.; Cross, J. B.; Bakken, V.; Adamo, C.; Jaramillo, J.; Gomperts, R.; Stratmann, R. E.; Yazyev, O.; Austin, A. J.; Cammi, R.; Pomelli, C.; Ochterski, J. W.; Ayala, P. Y.; Morokuma, K.; Voth, G. A.; Salvador, P.; Dannenberg, J. J.; Zakrzewski, V. G.; Dapprich, S.; Daniels, A. D.; Strain, M. C.; Farkas, O.; Malick, D. K.; Rabuck, A. D.; Raghavachari, K.; Foresman, J. B.; Ortiz, J. V.; Cui, Q.; Baboul, A. G.; Clifford, S.; Cioslowski, J.; Stefanov, B. B.; Liu, G.; Liashenko, A.; Piskorz, P.; Komaromi, I.; Martin, R. L.; Fox, D. J.; Keith, T.; Al-Laham, M. A.; Peng, C. Y.; Nanayakkara, A.; Challacombe, M.; Gill, P. M. W.; Johnson, B.; Chen, W.; Wong, M. W.; Gonzalez, C.; Pople, J. A. *Gaussian 03*, revision B.04; Gaussian, Inc.: Pittsburgh, PA, 2003.
- (23) Chin, W.; Dognon, J.-P.; Piuze, F.; Tardivel, B.; Dimicoli, L.; Mons, M. *J. Am. Chem. Soc.* **2005**, *127*, 707.
- (24) (a) Bhattacharya, A.; Guo, Y. Q.; Bernstein, E. R. *J. Phys. Chem. A* **2009**, *113*, 811. (b) Bhattacharya, A.; Guo, Y. Q.; Bernstein, E. R. *Acc. Chem. Res.* **2010**, *43*, 1476. (c) Soto, J.; Arenas, J. F.; Otero, J. C.; Pelaez, D. *J. Phys. Chem. A* **2006**, *110*, 8221. (d) Domcke, W.; Yarkony, D. R.; Koppel, H. *Conical Intersections: Electronic Structure, Dynamics and Spectroscopy*; World Scientific: Singapore, 2003.
- (25) Schatz, G. C.; Ratner, M. A. *Quantum Mechanics in Chemistry*; Prentice-Hall: Englewood Cliffs, NJ, 1993.
- (26) Remacle, F.; Levine, R. D. *Proc. Natl. Acad. Sci. U.S.A.* **2006**, *103*, 6793.